Chemical Structure and Thermochemical Properties of Enzymatically Acidolyzed Lignins from Soft and Hard Wood

Ji-Biao Li, Shu-Bin Wu,* and Xiao-Hong Li

Enzymatic/Mild Acidolysis Lignin (EMAL) was isolated from *Cunninghamia lanceolata* and eucalyptus woods. The chemical structure and thermochemical properties were characterized by means of elemental analysis, Fourier transform infrared spectroscopy (FT-IR), thermal gravimetric analysis (TG), and pyrolysis-gas chromatography combined with mass spectrometry (Py-GC/MS). The EMAL isolated from *Cunninghamia lanceolata* (C-EMAL) had larger HHV (higher heat value) in comparison to the EMAL isolated from eucalyptus (E-EMAL) due to the greater carbon content of the C-EMAL. The E-EMAL had more syringyl units, whereas the C-EMAL contained more guaiacyl units. It was observed that thermal decomposition occurred over a wide temperature range, and that at a given starting temperature, within the same sample, a higher heating rate produced a higher temperature at which maximum weight loss peaked. The pyrolysis products were mainly composed of carboxylic acids, alcohols, ketones, aldehydes, olefins, alkanes, esters, ethers, and phenols. At all pyrolysis temperatures, the largest components of the pyrolysis products obtained from C-EMAL were the phenols.

Keywords: Lignin; Elemental analysis; FT-IR; TG; Py-GC/MS

*Contact information: State Key Lab. Pulp & Paper Engineering, South China University of Technology Guangzhou, Guangdong, P R. China 510640; *Corresponding author: shubinwu@scut.edu.cn*

INTRODUCTION

With increasing concerns about environmental protection and the depletion of fossil fuels, the need for efficient utilization of biomass resources has attracted worldwide interest, as biomass has been recognized as a potential source of renewable energy to replace the declining fossil fuel resources (Demirbas 2002; Pattiya 2011). Currently, about 80 to 85% of the accumulated carbon dioxide in the atmosphere is attributed to the combustion of fossil fuels and land abuse, especially deforestation.

Focus has gradually turned to replacing fossil fuels with renewable ones to decrease the emissions of greenhouse gases. To achieve this shift to renewable fuels, new strategies and large-scale processes for production are needed. Biomass energy has become one of the most important ingredients in the sustainable energy system due to its renewability, abundance, and significant environmental benefits (Chauhan and Kaith 2012). Recently, many methods have been developed for biomass utilization, such as combustion (McIlveen-Wright *et al.* 2006.), pyrolysis (Lou *et al.* 2010; Lv *et al.* 2012), gasification (Lu *et al.* 2008; Zhang *et al.* 2012), and liquefaction (Saisu *et al.* 2003; Fang *et al.* 2008; Roberts *et al.* 2010).

Previous studies have focused on the thermochemical properties of biomass raw materials such as cellulose, hemicellulose, and other model compounds. Hazelnut shell

(Demirbas 2010) was liquefied in glycerol and glycerol Na_2CO_3 mixture and in water directly, and it was found that sodium carbonate could lead to the hydrolysis of macro-molecules, such as cellulose and hemicellulose, into smaller fragments, and the polar glycerol solvent molecules are attracted to the dry solid matrix and held by hydrogen bonding forces; The thermochemical conversion of catechol as a lignin model compound (Wahyudiono *et al.* 2009) was studied in supercritical water, and it was observed that phenol was considered as a main product of catechol decomposition and the formation of phenol increased with an increase in water density. However, research on lignin is scarce compared with the research that has been done on various other biomass materials. In this work, a method proposed by Wu *et al.* (2006) for obtaining enzymatic/mild acidolysis lignin (EMAL) from wood fiber was applied. This method efficiently contributed to the separation of chemical bonds between lignin and carbohydrate under mild chemical conditions. With the aim investigating the pyrolytic properties of lignin, this work will present information on the thermochemical characteristics of lignin and on the distribution of small molecular weight compounds as determined by TG and Py-GC/MS, which is of great guiding significance for revealing the pyrolysis mechanism of lignin.

EXPERIMENTAL

Materials

Eucalyptus and *Cunninghamia lanceolata*

Eucalyptus (species not identified) and *Cunninghamia lanceolata* woods were acquired from Guangdong Province (P. R. China). These two raw materials were ground using a disintegrator, and then extracted for 48 h using an acetone solvent and later ball-milled for at least 60 h. The obtained powder was used for the preparation of EMAL, which was conducted via isolation of the lignin from both kinds of wood.

Cellulase enzymatic hydrolysis

The milled wood powder (10 g on a dry basis) was subjected to enzyme treatment using an industrial cellulase (CMCase) with an activity of about 1,300 units/mL of carboxymethyl cellulose (CMC). The enzymatic hydrolysis was carried out at 40 ^{o}C in a 500-mL conical flask over a period of 48 h at a pH value of 4.5 (using an acetate buffer solution). After enzymatic hydrolysis, the impure enzymatic hydrolysis lignin was centrifuged and washed twice with acidic deionized water having a pH value of 2.0 (HCl) and then freeze-dried for 24 h.

Mild acidolysis

Impure enzymatic hydrolysis lignin (5 g on a dry basis) was suspended in 100 mL of dioxane/acidified deionized water solution (85:15 v/v, 0.01 mol/L HCl) and was extracted at 87 ^{o}C in a nitrogen gas atmosphere for 2 h. The obtained mixture solution was filtered, and the lignin solution was collected. The solid residue was sequentially washed with fresh dioxane/deionized water solution (85:15 v/v) 2 to 3 times. Next, the entire filtrated solution was neutralized with sodium bicarbonate under magnetic stirring that lasted 3 h. The neutralized solution was then evaporated until a thick solution had formed. This thick solution was carefully dropped into a large quantity of acidified deionized water (pH 2.0, HCl), and the precipitated lignin was separated by centrifugation, then washed and freeze-dried. Finally, the obtained lignin was washed

with HPLC-grade hexane and dried in a vacuum oven at room temperature.

Methods

Characterization of EMAL chemical structure

The elements of the EMAL isolated from eucalyptus and *Cunninghamia lanceolata* were analyzed using a Vario-EL CUBE elemental analyzer (Germany ELEMENTAR), and an FT-IR spectra of the EMAL was recorded on a Nexus 670 spectrophotometer (Thermo Nicolet) from 4,000 to 500 cm^{-1} using a KBr disc containing 1% finely ground samples.

Thermochemical properties of EMAL

A thermogravimetric experiment was performed using a TG209 integrated Thermal Gravimetric Analyzer from NETZSCH Corporation in Germany with high purity nitrogen with a flow rate of 25 mL/min as the carrier gas. About 8 to 10 mg of material was placed in a ceramic crucible and then heated from room temperature to 700 ^{o}C at a heating rate of 10 ^{o}C/min and 20 ^{o}C/min. The obtained thermogravimetric rate data were automatic saved through the system of the gravimetric analyzer.

The Py-GC/MS systems included a JHP-3 JAI Curie point pyrolyzer (CDS5200, USA) and a Shimadzu QP2010 Plus gas chromatograph/mass spectrometer (Japan). About 0.1 mg of each of the EMAL samples was pyrolyzed at 400, 500, and 600 ^{o}C for 15 s, and the gas products were then purged by high-purity helium into the gas chromatograph via a transfer line. The flow rate of the carrier gas was 50 mL/min, and the split ratio was 30:1. The injection temperature was 280 ^{o}C. The pyrolysis products were separated in a DB-5 (Agilent Technologies, USA) capillary column (15 m × 0.25 mm × 0.25 μm). For lignin pyrolysis, the GC oven was kept at 50 ^{o}C for 2 min and then heated to 250 ^{o}C at steps of 10 ^{o}C/min. The ion source temperature was 250 ^{o}C. The mass spectrometer was operated in the EI mode using 70 eV of electron energy. The mass range m/z 45 to 500 was scanned. An identification of the pyrolysis compounds was attained by comparison of their mass fragment with the PerkinElmer NIST 05 mass spectral library.

RESULTS AND DISCUSSION

Elemental Analysis

The C, H, N, and S contents were determined using the elemental analyzer. The O content was calculated by subtracting the sum of the C, H, N, and S contents from 100%. Results for the elemental analysis of the two kinds of EMAL are summarized in Table 1. The higher heating value (HHV) of the biomass was calculated using the Dulong formula (Yuan *et al.* 2009),

$$HHV\ (MJ/kg) = 0.3383Z_C + 1.422(Z_H - Z_O/8) \quad (1)$$

where Z_C, Z_H, and Z_O are the weight percentages of carbon, hydrogen, and oxygen, respectively. Generally, the HHV was strongly related to the carbon content, such that greater carbon content led to a greater HHV of the biomass. From Table 1, it can be seen that the C-EMAL had a larger HHV in comparison to the E-EMAL, a difference that was attributed to the larger carbon content of the C-EMAL.

Table 1. Elemental Analysis of EMAL (%)

Materials	Elements					HHV (MJ/Kg)
	C	H	O	N	S	
E-EMAL	57.88	6.625	34.813	0.14	0.542	22.814
C-EMAL	60.31	6.546	32.238	0.24	0.666	23.981

FT-IR Analysis

The FT-IR spectra of the two EMALs are shown in Fig. 1. The IR signal and the typical absorption with the corresponding functional groups are listed in Table 2. It can be observed that the FT-IR spectra of E-EMAL and C-EMAL were generally similar, only with different absorption intensities. The absorption signals of the C-EMAL at 3422, 2928, 1656, and 1263 cm^{-1} were larger and broader, which suggested that the C-EMAL contained more conjugated C=O compounds and more guaiacyl units. On the other hand, the signal of the E-EMAL at 1123 cm^{-1} was sharper and stronger, meaning that the E-EMAL contained more syringyl units.

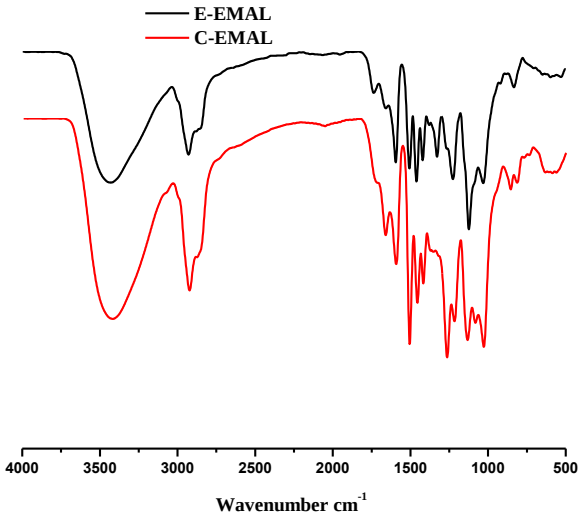

Fig. 1. FT-IR spectra of E-EMAL and C-EMAL

Table 2. Analysis of FT-IR Spectra of EMAL

Wave number(cm^{-1})		Functional groups	Origin
E-EMAL	C-EMAL		
3429	3422	O-H stretching	Phenolics
2920, 2850	2928, 2847	C-H stretching	$-CH_3$,$-CH_2$,-CH
1710	1708	C=O stretching	Non-conjugated carbonyl
1656	1656	C=O stretching	Conjugated carbonyl
1594, 1506, 1421	1596, 1509, 1422	C=C stretching	Aromatic ring
1461	1460	C-H bending	$-CH_2$
1251	1263	=C-O-R stretching	Guaiacyl unit
1123	1128	C-H bending	Syringyl unit
1022	1028	C-H bending, C-O bending	Aromatic ring, Methoxyl group
825	848	C-H bending	Guaiacyl unit

TG Analysis

The TG and DTG curves of the E-EMAL and C-EMAL at the heating rates of 10, and 20 ^{o}C/min are shown in Figs. 2, 3, 4, and 5, respectively. These figures showed that thermal decomposition occurred over a wide temperature range, arising at approximately 150 ^{o}C. Then, a major loss of weight followed, accompanied by liquefaction with charring, which was highly exothermic (Grabowska *et al.* 2013). However, beyond 500 ^{o}C, this was followed by a slow additional mass loss leading up to the final temperature, at which point the TG curves tended to become flat. It was seen that the char residue at 700 ^{o}C for E-EMAL varied between 25 and 30% at the heating rate of 10, and 20 ^{o}C/min respectively, whereas the char residue at 700 ^{o}C for C-EMAL rose from 30 to 35% Depending on the heating rates, these thermochemical differences resulted in different chemical structures of the two EMALs. C-EMAL contained more guaiacyl units, which contributed to condensation and coupling reaction and then led to the higher char residue (Wang *et al.* 2009).

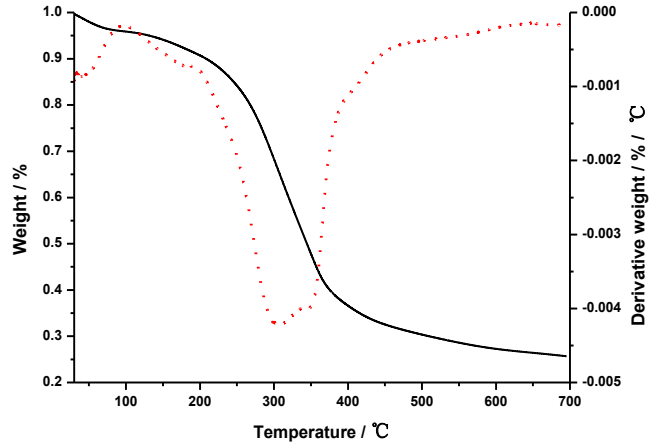

Fig. 2. TG and DTG curves of E-EMAL at 10 ^{o}C/min

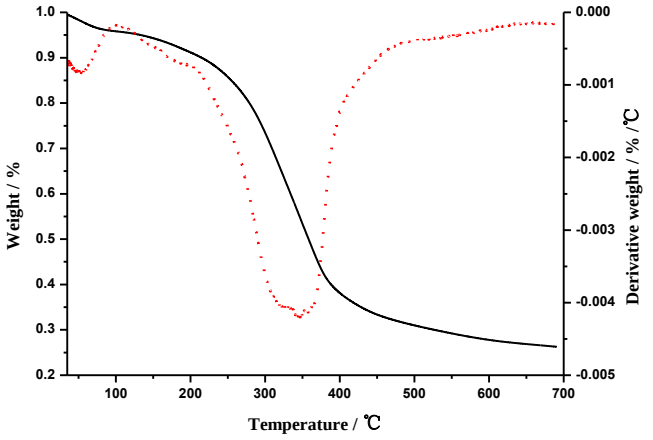

Fig. 3. TG and DTG curves of E-EMAL at 20 ^{o}C/min

It was also observed that, at a given starting temperature within the same sample, higher heating rates resulted in a higher temperature for maximum weight loss. This could have been because the increased heating rate resulted in shortening of the time that was required to attain the temperature necessary for pyrolysis, thus favoring thermal degradation while also bringing about larger differences in temperature between the

internal and external parts of sample particles and postponing the conduct of heat transfer. This would have affected the pyrolysis of the external parts, elevating the temperature of the maximum weight loss peak.

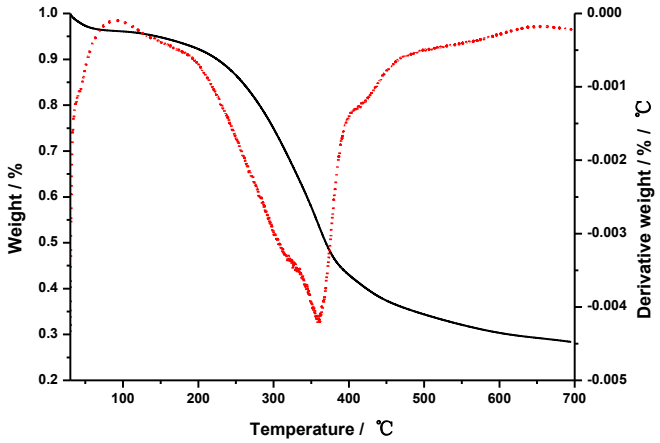

Fig. 4. TG and DTG curves of C-EMAL at 10 °C/min

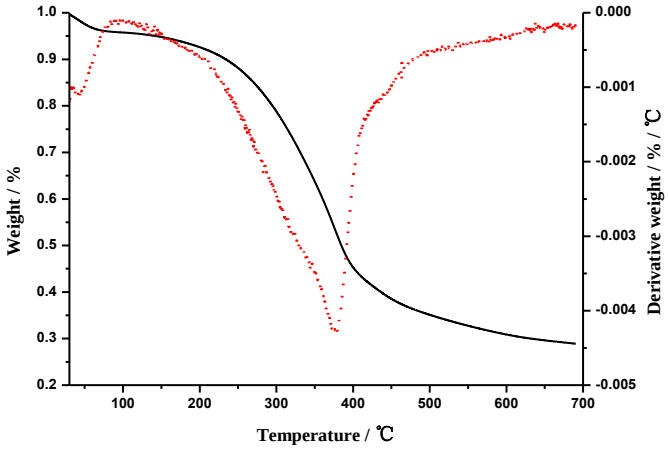

Fig. 5. TG and DTG curves of C-EMAL at 20 °C/min

Py-GC/MS Analysis

The total ion chromatograms of E-EMAL and C-EMAL are shown in Figs. 6 and 7. Results of analysis of the pyrolysis products at 400, 500, and 600 °C are presented in Tables 3 and 4. The distribution laws for the main pyrolysis products of the two EMALs and shown in Figs. 8 and 9.

In accordance with Figs. 6 and 7 and Table 3 and 4, it was concluded that the diversity and content of the pyrolysis products varied between the two EMALs, and the number of proton peak increased as the pyrolysis temperature rose, which indicated that the amount of pyrolysis product increased as well. It was also observed that the amount of pyrolysis product of C-EMAL during the retention time of 10 to 15 min was much more than that during any other retention time at 400, 500, and 600 °C, while only for E-EMAL at 600 °C, these phenomena might be attributed to the differences in chemical structure between C-EMAL and E-EMAL.

Figures 8 and 9 showed that the pyrolysis organic products of the two EMALs were mainly composed of carboxylic acids, alcohols, ketones, aldehydes, olefins, alkanes, esters, ethers, and phenols at 500 and 600 ^{o}C. Among these, the largest components of the pyrolysis products of C-EMAL at the pyrolysis temperatures of 400, 500, and 600 ^{o}C were the phenols, constituting approximately 25.37%, 39.62%, and 30.4%, respectively. Unlike C-EMAL, the largest components of the pyrolysis products of E-EMAL varied depending on temperature; the acids accounted for 16.17% at 400 ^{o}C; the ethers for about 41.78% at 500 ^{o}C, and the phenols for about 27.18% at 600 ^{o}C. The advent of phenol and some other phenols with low molecular weight at 600 ^{o}C was attributed to the secondary pyrolysis (Nakamura *et al.* 2008).

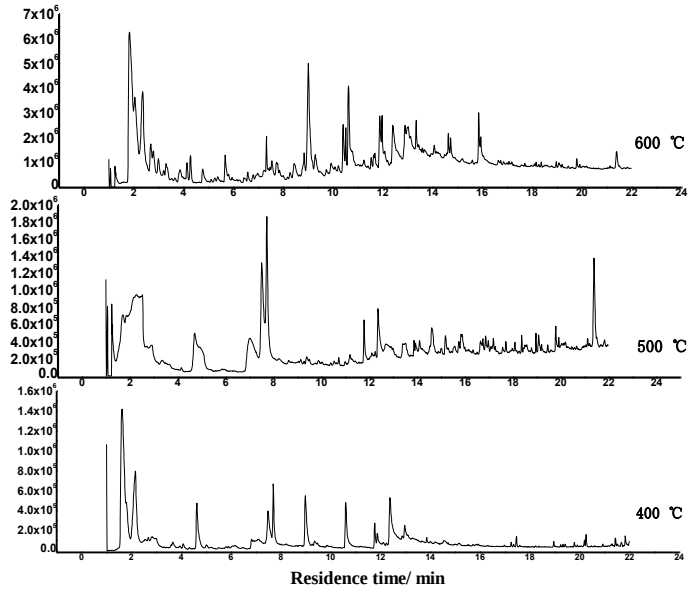

Fig. 6. Total ion chromatograms of E-EMAL pyrolysis at 400, 500, and 600 ^{o}C

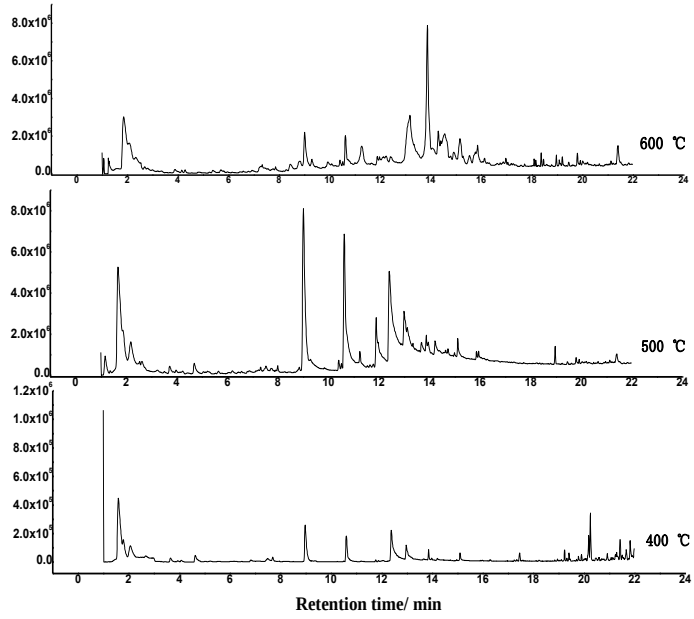

Fig. 7. Total ion chromatograms of C-EMAL pyrolysis at 400, 500, and 600 ^{o}C

Tables 3 and 4 showed that the pyrolysis products of phenols of the two EMALs mainly contained cresyl (H-type), guaiacyl (G-type), and syringyl (S-type) compounds.

Table 3. Analysis of Pyrolysis Products of E-EMAL at 400, 500, and 600 °C

Groups	Compound	Molecular weight	Area %		
			400°C	500°C	600°C
Alcohols	3-Butyn-1-ol	70	-	1.95	0.38
	1-Cyclohexene-1-methanol	112	-	3.74	0.78
	2-Methyl-1-pentanol	102	-	-	9.43
	Ethylene glycol	62	2.20	-	-
	1,3-Dioxolane-2-methanol	104	-	-	2.55
	1-nonanol	144	-	-	1.70
	(4-isopropylphenyl) methanol	150	-	1.18	-
Acids	D-Alanine	89	-	3.75	-
	Acetic acid glacial	60	15.94	-	10.45
	Pentadecanoic acid	242	-	1.57	-
	Stearic acid	284	0.23	-	-
Furans	Furfuryl alcohol	98	0.72	0.61	-
	Tetrahydrofuran	72	-	1.09	-
	Furfural	96	5.69	3.71	0.64
Ethers	1-Ethoxy-2-methylpropane	102	-	-	2.14
	2-Ethoxyethanol	90	-	-	0.65
	2-(Vinyloxy)ethanol	88	-	-	0.83
	1-Ethoxy-2-methylpropane	102	-	-	0.39
	2-Ethoxyethyl ether	162	-	-	1.08
	2-(2-Methoxyethoxy)ethanol	120	-	-	0.33
	Diethylene glycol	106	-	9.30	-
	2(2-Ethoxyethoxy)ethanol	134	5.25	12.80	-
	12-Crown-4	176	5.10	19.34	-
	Di(ethylene glycol) vinyl ether	132	-	-	0.96
	Octadecyl vinyl ether	296	-	0.34	-
Olefins	1-Octene	112	-	-	0.65
	1-Decene	140	-	-	1.17
	1-Tridecene	182	-	-	1.15
	1-Tetradecene	196	-	-	3.60
	alpha-Cedrene	204	-	0.55	-
	1-Pentadecene	210	-	-	0.63
	1-Nonadecene	267	-	1.13	1.64
Aldehydes	Decanal	156	-	0.52	-
	Pentadecanal	226	0.21	-	-
	4-Isopropylbenzaldehyde	148	1.93	2.63	-
	4-Isopropylbenzaldehyde	148	-	0.45	-
	Vanillin	152	-	2.87	-
	3,5-Dimethoxy-4-hydroxybenzaldehyde	182	-	0.80	-
	Hexadecanal	240	-	0.62	-
Phenols	o-Cresol	108	-	-	1.24
	Guaiacol	124	-	-	8.76
	2-Methoxy-4-methylphenol	138	4.88	-	-
	4-Ethyl-2-methoxyphenol	152	1.23	-	-
	4-Hydroxy-3-methoxystyrene	150	6.36	-	-
	2,6-Dimethylphenol	122	-	-	1.32
	2-Methoxy-5-methylphenol	138	-	-	6.62
	2,3,5-Trimethylphenol	136	-	-	0.87
	4-Ethyl-2-methoxyphenol	152	-	-	0.37
	4-Ethyl-2-methoxyphenol	152	-	-	2.37

	2,6-Dimethoxyphenol	154	0.26	-	1.86
	2-Methoxy-3-(2-propenyl)phenol	164	1.44	0.42	-
	2-Methoxy-5-[(E)-1-propenyl]phenol	164	-	-	2.84
	2-methoxy-4-propyl-Phenol	166	0.20	-	1.29
	(Z)-Isoeugenol	164	-	0.54	-
	3-Methoxy-2-naphthol	174	-	1.10	-
	2,6-Dimethoxy-4-(2-propenyl)phenol	194	-	0.75	-
Alkanes	Hexadecane	226	-	-	1.20
	Pentadecane	212	-	-	0.90
	Heptadecane	240	-	-	0.78
Ketones	5-Hexen-2-one	98	5.68	-	-
	Hydroxyacetone	74	0.66	-	-
	2-Methyl-4-hydroxyacetophenone	150	-	-	2.36
	Acetovanillone	166	0.48	2.68	-
	(4-Hydroxy-3-methoxyphenyl)acetone	180	-	1.88	-
	1-(2,4-Dihydroxy-3-methylphenyl)-1-propanone	180	-	2.02	-
Esters	Ethyl pipecolinate	157	0.49	-	-
	Hexadecyl octanoate	368	-	0.35	-
	Diisobutyl phthalate	278	0.36	0.66	-
	Dibutyl phthalate	278	0.20	0.35	-
	2-ethylhexyl hydrogen phthalate	278	-	7.37	0.79
Others	Toluene	92	-	-	0.69
	CO_2	44	30.31	-	18.08
	Benzothiazole	135	-	0.36	-
	L-Nicotine	162	-	3.66	-
	3,5-Dimethoxytoluene	152	-	-	0.51
	Dicyclohexylamine	181	-	0.68	-
	N,N-Dimethylpropionamide	101	0.17	-	-
	4-Methylbenzyl chloride	140	0.13	-	-
	2-Phenylnaphthalene	204	0.33	-	-
	1-Benzylnaphthalene	218	0.42	-	-
	1-Benzylnaphthalene	218	0.27	-	-
	p-Terphenyl	230	0.48	-	-

Table 4. Analysis of Pyrolysis Products of C-EMAL at 400, 500, and 600 ^{o}C

Groups	Compound	Molecular weight	Area %		
			400^{o}C	500^{o}C	600^{o}C
Ketones	2-Butanone	72	-	4.05	-
	Hydroxyacetone	74	-	0.93	-
	4-Hydroxy-3-methylacetophenone	150	-	15.21	3.94
	(4-Hydroxy-3-methoxyphenyl)acetone	180	-	-	4.02
	Acetovanillone	166	-	-	6.26
Alcohols	Cyclobutanol	72	-	-	4.01
	Decyl alcohol	158	-	0.28	-
	1-Undecanol	172	-	2.79	0.70
	1-pentadecanol	228	-	-	0.34
	Cedrol	222	-	-	0.58
	3-cyclohexyl-1-propanol	142	0.42	-	-
Acids	Acetic acid glacial	60	6.37	4.68	-
	Acetoxyacetic acid	118	-	0.46	-
	Decanoic acid	172	0.58	-	-
	1-Naphthalenyloxyacetic acid	202	0.67	-	-
	Myristic acid	228	-	-	0.12
	Pentadecanoic acid	242	-	0.24	0.81
Furans	Furfural	96	1.14	0.74	-

	5-Methyl furfural	110	-	0.27	-
	6-methoxy-3-methyl-benzofuran	162	-	-	3.77
Phenols	Phenol	94	-	-	0.55
	o-Cresol	108	-	-	1.40
	Guaiacol	124	10.32	13.14	5.39
	2-Methoxy-4-methylphenol	138	5.24	-	-
	2-methoxy-5-methyl-phenol	138	-	11.05	2.84
	4-Ethyl-2-methoxyphenol	152	-	2.50	0.78
	2-methoxy-3-(2-propen-1-yl)-phenol	164	-	-	2.20
	4-Hydroxy-3-methoxystyrene	150	9.81	0.74	-
	Eugenol	164	-	4.27	-
	2-methoxy-4-propyl-Phenol	166	-	4.12	-
	(Z)-Isoeugenol	164	-	1.92	-
	(e)-isoeugenol	164	-	1.88	17.24
Olefins	1-Decene	140	-	-	0.23
	(R)-4-Isopropenyl-1-methyl-1-cyclohexene	136	-	0.22	-
	1-Tridecene	182	-	0.15	0.20
	1-Tetradecene	196	-	1.23	1.55
	alpha-Cedrene	204	1.14	1.11	-
	1,1-Diphenylethylene	180	0.22	-	-
	4-Phenyl-1-butene	132	1.12	-	-
	1-Heptadecene	238	-	0.97	-
	1-Nonadecene	267	-	0.24	0.31
Ethers	triethylene glycol ethyl ether	178	-	0.42	-
	Di(ethylene glycol) vinyl ether	132	-	0.38	-
	3-Methylanisole	122	-	-	0.17
	2,5-Dimethylphenol methylether	136	-	1.43	0.94
	Isohomoveratrol	152	-	0.47	-
	Methyl isoeugenol	178	-	-	0.65
	1-Ethoxydodecane	214	-	-	0.32
	12-Crown-4	176	0.67	-	-
	Octadecyl vinyl ether	297	1.13	-	0.34
Aldehydes	4-Isopropylbenzaldehyde	148	-	0.13	-
	4-Hydroxy-2-methoxybenzaldehyde	152	-	-	13.88
	Pentadecanal	226	0.90	-	-
	Hexadecanal	240	-	-	0.64
Alkanes	Tetradecane	198	-	0.55	-
	Pentadecane	212	-	0.59	-
	Heptadecane	240	-	0.23	-
	Heneicosane	297	-	--	0.26
Esters	Methyl pyruvate	102	-	0.16	-
	4-Allyl-2-methoxyphenyl acetate	206	3.00	-	-
	Diisobutyl phthalate	278	0.19	0.42	0.51
	Methyl vanillate	182	-	-	1.19
	Dibutyl phthalate	278	-	-	0.29
	2-ethylhexyl hydrogen phthalate	278	-	0.42	1.81
Others	Toluene	92	-	-	0.29
	CO_2	44	27	12.88	12.02
	Dicyclohexylamine	181	-	1.29	-
	Cyclobutylamine	71	6.75	-	-
	2-Phenylnaphthalene	204	3.41	-	-
	1-Benzylnaphthalene	218	2.60	-	-
	1-Benzylnaphthalene	218	1.67	-	-
	p-Terphenyl	230	2.64	-	-

Lignin macromolecules consisted of a large number of β-O-4 and α-O-4 couplings (Pandey and Kim 2011) which were easy to cleave as the pyrolytic temperature increased, accompanied with the advent of H-, G-, and S-type phenols; Meanwhile, the cleavages of β-O-4 and C_α-C_β at high temperature contributed to the formation of acetic acid, and the rupture of aromatic rings resulted in straight-chain alkanes.

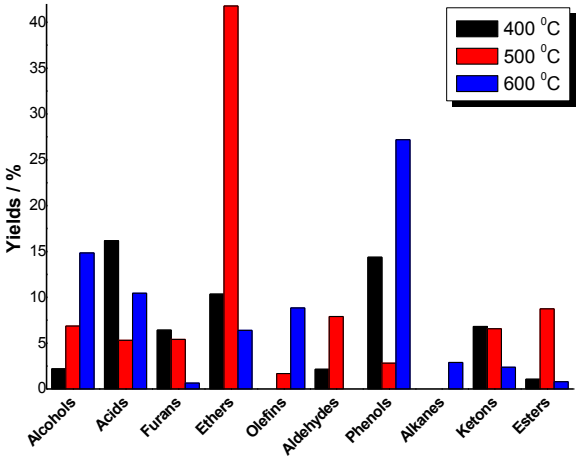

Fig. 8. The distribution law of the main pyrolysis products of E-EMAL at 400, 500, and 600 °C

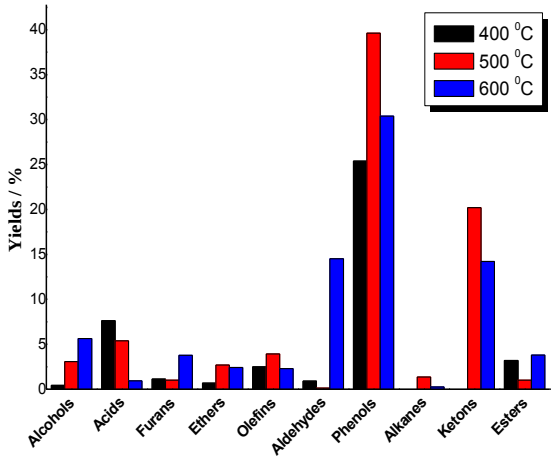

Fig. 9. The distribution law of the main pyrolysis products of C-EMAL at 400, 500, and 600 °C

CONCLUSIONS

1. Enzymatic/mild acidolysis lignin from *Cunninghamia lanceolata* (C-EMAL) was found to have a larger higher heating value (HHV) than the corresponding lignin from eucalyptus (E-EMAL) due to the greater carbon content of the C-EMAL.
2. C-EMAL contained more conjugated C=O compounds and more guaiacyl units, whereas, given that the signal of E-EMAL at 1123 cm^{-1} was sharper and stronger, the E-EMAL included more syringyl units.

3. Thermal decomposition occurred over a wide temperature range, beginning at approximately 150 ^{o}C and followed by a slow additional mass loss leading up to the final temperature. The TG curves tended to become flat beyond 500 ^{o}C. It was also observed that, at a given starting temperature within the same sample, higher heating rates led to a higher temperature for peak weight loss.
4. The diversity and content of the pyrolysis products varied between the two EMALs and the pyrolysis organic products of the two EMALs were mainly composed of carboxylic acids, alcohols, ketones, aldehydes, olefins, alkanes, esters, ethers, and phenols at 500, and 600 ^{o}C. The largest components of the pyrolysis products of the C-EMAL were the phenols, constituting approximately 25.37% at 400 ^{o}C, 39.62% at 500 ^{o}C, and 30.4% at 600 ^{o}C. These phenols mainly consisted of guaiacol and some other phenolic derivatives. Unlike those of C-EMAL, the largest components of the pyrolysis products of E-EMAL varied depending on temperature: acids accounted for 16.17% at 400 ^{o}C, ethers for 41.78% at 500 ^{o}C, and phenolics for 27.18% at 600 ^{o}C.

ACKNOWLEDGEMENTS

This work was supported by the State Natural Sciences Foundation (NO.31270638) and the National Major Fundamental Research Program of China (973 programs, NO.2013CB228101).

REFERENCES CITED

Chauhan, A., and Kaith, B. (2012). "Novel materials procured from surface modification of biomass," *Waste and Biomass Valor*. 3(2), 141-148.

Demirbas, A. (2002). "Partly chemical analysis of liquid fraction of flash pyrolysis products from biomass in the presence of sodium carbonate," *Energy Conversion and Management* 43(14), 1801-1809.

Demirbas, A. (2010). "Direct and alkaline glycerol liquefaction of hazelnut shell," *Energy Sources*, *Part A* 32 (8), 744-751.

Fang, Z., Sato, T., Smith, Jr., R. L., Inomata, H., Arai, K., and Kozinski, J. A. (2008). "Reaction chemistry and phase behavior of lignin in high-temperature and supercritical water," *Bioresour. Technol.* 99(9), 3424-3430.

Grabowska, B., Szucki, M., Suchy, J. S., and Eichholz, S. (2013). "Thermal degradation behavior of cellulose-based material for gating systems in iron casting production," *Polimery* 58(1), 39-44.

Lu, Y. J., Jin, H., Guo, L. J., Zhang, X. M., Cao, C. Q., and Guo, X. (2008). "Hydrogen production by biomass gasification in supercritical water with a fluidized bed reactor," *Int. J. Hydrogen Energy* 33(21), 6066-6075.

Lou, R., Wu, S. B., and Lv, G. J. (2010). "Fast pyrolysis of enzymatic/mild acidolysis lignin from moso bamboo," *BioResources* 5(2), 827-837.

Lv, G. J., and Wu, S. B. (2012). "Analytical pyrolysis studies of corn stalk and its three main components by TG-M S and Py-GC/MS," *J. Anal. Appl. Pyrolysis* 97, 11-18.

McIlveen-Wright, D. R., Pinto, F., Armesto, L., Caballerod, M. A., Aznard, M. P., Cabanillasc, A., Huanga, Y., Francob, C., Gulyurtlub, I., and McMullana, J. T. (2006).

"A comparison of circulating fluidized bed combustion and gasification power plant technologies for processing mixtures of coal, biomass and plastic waste," *Fuel Process. Technol*. 87(9), 793-801.

Nakamura, T., Kawamoto, H., and Saka, S. (2008). "Pyrolysis behavior of Japanese cedar wood lignin studied with various model dimers," *J. Anal. Appl. Pyrolysis* 81(2), 173-182.

Pandey, M. P., and Kim, C. C. (2011). "Lignin depolymerization and conversion: A review of thermochemical methods," *Chem. Eng. Technol.* 34, 29-41.

Pattiya, A. (2011). "Bio-oil production via fast pyrolysis of biomass residues from cassava plants in a fluidized-bed reactor," *Bioresour. Technol.* 102(2), 1959-1967.

Roberts, V., Rendt, S., Lemonidou, A. A., Li, X. B., and Lercher, J. A. (2010). "Influence of alkali carbonates on benzyl phenyl ether cleavage pathways in superheated water," *Appl. Catal. B.* 95(1-2), 71-77.

Saisu, M., Sato, T., Watanabe, M., Adschiri, T., and Arai, K. (2003). "Conversion of lignin with supercritical water-phenol mixtures," *Energy Fuels* 17(4), 922-928.

Wu, S. B., and Li, M. S. (2006). "Study on chemical structure characteristics of wheat straw lignin from enzymatic hydrolysis acidolysis," *Chemistry and Industry of Forest Products* 26(1), 105-111.

Wahyudiono, Sasaki, M., and Goto, M. (2009). "Conversion of biomass model compound under hydrothermal conditions using batch reactor," *Fuel* 88, 1656-1664.

Wang, S. R., Wang, K., Liu, Q., Gu, Y. L., Luo, Z. Y., Cen, K. F., and Fransson, T. (2009). "Comparison of the pyrolysis behavior of lignins from different tree species," *Biotechnol. Adv.*27 (5), 562-567.

Yuan, X. Z., Tong, J. Y., Zeng, G. M., Li, H., and Xie, W. (2009). "Comparative studies of products obtained at different temperatures during straw liquefaction by hot compressed water," *Energy Fuels* 23, 3262-3267.

Zhang, Z., Chen, B., Chen, A., and Zhao, W. (2012). "Barriers to commercialization development of crop straw gasification technology in China and promoting policy design," *Energy Sources Part B* 8(3), 279-289.

Article submitted: May 27, 2013; Peer review completed: August 19, 2013; Revised version received and accepted: August 19, 2013; Published: August 20, 2013.